POSTER SESSION n°1

Presentation on
Wednesday 10 May 12:00-12:30

by Dr. Jian-Rong Gao

Poster session n°1 from 14:00 to 15:30

VO_2 TES as Room Temperature THz Detectors

Biddut K. Banik, Harald F. Merkel

Abstract— **VO_x materials hold very high potential to be used as room temperature bolometer. A brief review on room temperature bolometers and VO_x characteristics is presented. The hysteretic metal-insulator transition behavior of a VO_x microbolometer has been investigated. An algebraic hysteresis model has been used to model the resistance-temperature characteristic of the bolometer. The magnetic limiting loop proximity (L^2P) hysteresis theory is modified to represent the VO_x major and minor hysteresis loops. The responsivity of the bolometer is also calculated. Loop accommodation process is explained. Nonsymmetrical hysteretic behavior has also been discussed.**

Index Terms— **Bolometers, hysteresis, vanadium oxide.**

I. Introduction

TODAY THz detectors are exclusively based on superconducting materials. Superconducting Tunnel Elements (SIS), Transition Edge Sensors (TES) have been used as direct detectors while Hot Electron Bolometers (HEB) has been used for heterodyne receivers without frequency limitations. These sensors have become standard solutions for radioastronomy and other remote sensing applications. In recent years, security and safety applications have emerged as potentially new applications for THz technology. Proposed systems (e.g. airport security, standoff checkpoints) for detection of explosives and concealed weapons require imaging and detection at some 20 m distance. Compared to radioastronomic applications, the requirements on spectroscopic resolution are here greatly relaxed. Interesting molecular lines are temperature and pressure-widened. Imaging is crucial, so any commercially interesting detector system must be capable to be extendable to 100s and 1000s of pixels. Commercially viable systems must operate at room temperature or even better at elevated temperature levels. The advantages of uncooled sensors include no cryogenics, and no related complicated problems including additional power requirements, thermal shielding, and limited lifetime and additional weight and bulk. The results of such a basic study are presented in this work. Room temperature THz detection using composite bolometers, nanowires and nanotechnology, antenna coupled quasi-optical systems, superconducting TES devices having high T_c (YBaCuO) have been reported. Being used in military applications in the Near Infrared and having a very good potential as direct-detection detector, the use of vanadium oxides (VO_x) for room temperature THz detection is still virtually unexplored.

Vanadium oxide materials exhibit so-called Magnéli phase transition (i.e. between a metallic and semiconducting state) typically located at 68 °C, for the case of VO_2. Location and steepness of the transition temperature of VO_x films can be modified by varying process parameters as annealing temperature (in a sol-gel process) or doping the vanadium oxide with other cations or alternatively having a stochiometrically inaccurate mixture of VO_2 and V_3O_4.

Manuscript received May 11, 2006.

B. K. Banik is with the Dept. of Microtechnology and Nanoscience, Microwave Electronics Laboratory, MC2, Chalmers University of Technology; Göteborg, Sweden (e-mail: biddut.banik@mc2.chalmers.se).

H. F. Merkel is with the Dept. of Microtechnology and Nanoscience, Microwave Electronics Laboratory, MC2, Chalmers University of Technology and Food Radar AB, Göteborg, Sweden (e-mail: harald.merkel@mc2.chalmers.se).

II. Room Temperature Bolometers

A. A brief review

YBaCuO thin film bolometer for uncooled infrared detection has already been investigated [1] where YBaCuO on a Si substrate with and without a MgO buffer layer, and on an oxidized Si substrate with and without a MgO buffer layer were characterized. TCRs for all the films were greater than 2.5% K^{-1}. The highest TCR of 4.02% K^{-1} was observed on the amorphous YBaCuO thin film deposited on MgO/Si without a SiO_2 layer. YBaCuO bolometers have a responsivity as high as 3.8×10^5 V/W and a detectivity as high as 1.6×10^9 cm $Hz^{1/2}$/W for 1 μA bias current and frame frequency of 30 Hz if integrated with a typical air-gap thermal isolation structure. Microbolometers have been fabricated using a thin niobium film [2] as the detector element to operate at room temperature. The reported responsivity was up to 21 V/W at a bias of 6.4 mA, and electrical noise equivalent powers (NEP) of as low as 1.1 x 10^{-10} W/√Hz at 1 kHz. Metal bolometers at room temperature made of Pt, Au, Bi, and Ni have also been investigated [3].

B. VO_x Bolometers

Vanadium oxide thin films have been adopted [4] to make a 320 x 240 pixel IR detector and the reported NETD (noise equivalent temperature difference) was smaller than 0.1K at 60 Hz frame rate. The reported TCR is -1.64%/K and thermal time constant is 12 ms. VO_x thin film bolometers have been investigated and characterized by few other research groups [5, 6]. $V_2O_5/V/V_2O_5$ multilayer vanadium oxide thin films have been fabricated with high temperature coefficient [7]. Another 160 x 128 uncooled infrared sensor array was reported where calculated NETD for 4.25V bolometer bias and 2.74% TCR is 72 mK with f/1.8 optics [8]. A 16 x 16 array has been reported having responsivity of 1200 V/W, a detectivity of 2.2x10 cm$Hz^{1/2}$/W and NETD of 200 mK at 0.5 Hz frame rate [9].

III. VANADIUM OXIDE

A. VO_x characteristics

Several oxides of vanadium, such as VO, V_2O_3, VO_2, V_3O_5, V_6O_{13}, and V_2O_5, undergo a transition from a metal to a semiconductor or insulator phase at a critical temperature. VO_2 undergoes this transition near 68 °C as it transforms from a monoclinic to a tetragonal crystal structure, accompanied by large changes in electrical and optical behavior.

The phase transition properties make VO_x suitable for fabrication of a variety of electrical and optical devices, including electrical switching elements, thermistor thermal relays and optical switching elements. VO_x materials were used as intelligent window coatings [10]. Metal-insulator transition mechanism has been investigated [11]. The temperature and strain dependence of VO_x film resistance was also investigated [12]. Vanadium oxide films exhibit some interesting optical properties such as optical birefringence, electrochromism or optical switching [13]. The nature of the condensed phases formed upon hydrolysis and condensation.

The electrical and optical properties of VO_x largely depend on the derivation or deposition process, process temperature, ambient temperature, pressure, Stoichiometric composition, doping, grain size, type of substrate, specific orientation on its substrate [14-21]. Hysteresis width down to 1K has been reported [22]. Electrical and infrared properties of Vanadium Oxide nanocrystalline powder and thin films have been investigated [23].

Large negative temperature coefficients of resistance for high quality films have been reported [24]. Present uncooled VO_x bolometers are operated in the nonhysteretic metallic part of its resistance-temperature (R–T) curve, at temperatures below the metal-insulator (M–I) transition.

IV. VO_x CHARACTERIZATION

A. Hysteresis modeling

The magnetic limiting loop proximity (L^2P) hysteresis theory is modified to represent (1) the major hysteresis loops [25] where *Ms* is the saturation value, *Hc* is coercivity field, h_0 is a material dependent constant and δ is a sign operator.

$$M(H) = \frac{2}{\pi} Ms \arctan \frac{H - \delta Hc}{h_0} \tag{1}$$

It should be mentioned that (1) represents only the major hysteresis curve. To represent any arbitrary point (*H, M*) and to incorporate minor loops, (1) has been modified by [25].

$$M(H) = \frac{2}{\pi} Ms \arctan \frac{H_{pr} P(x) - \delta Hc + H}{h_0} \tag{2}$$

$$x = \frac{H - H_r}{H_{pr}} \tag{3}$$

Where, H_{pr} is the proximity field at reversal point H_r, and *P(x)* is the proximity function. *P(x) = 1-sinξx* for $2\xi x < \pi$ and *P(x)* = 0 otherwise. Here ξ and h_0 are material dependent constants.

The temperature dependent resistivity of VO_x bolometer can be represented as (4) where *Rs* is the saturation value of *R(T)* at high temperature end, χ and ψ are dependent on the saturation value of *R(T)* at low temperature end and on *R-T* slope, *υ(T)* incorporates the hysteresis loop, *w* is the hysteresis width, β_g represents the slope of *υ(T)*, *Tc* is the critical temperature and δ = sign(*dT/dt*). $\beta_g = \beta_{g+}$ for $\delta = 1$ and $\beta_g = \beta_{g-}$ for $\delta = -1$. Typically $\beta_{g+} = \beta_{g-}$ for VO_x materials but the values are different for doped VO_x, for instance, as β_g becomes dependent on δ and *T* [13].

$$R(T) = Rs + \chi \exp\left[\frac{\psi}{T + 273}\right] \upsilon(T) \tag{4}$$

$$\upsilon(T) = 0.5\left[1 + \tanh \beta_g \gamma\right] \tag{5}$$

$$\gamma = \delta \frac{w}{2} + Tc - T \tag{6}$$

Fig. 1 demonstrates *υ(T) and R(T)* for *Tc*= 68 °C, $\beta_g = \beta_{g+} = \beta_{g-} = 0.2$, *w*=6.5 °C, χ = *20 and* ψ=*2500* and *Rs* = *120.*

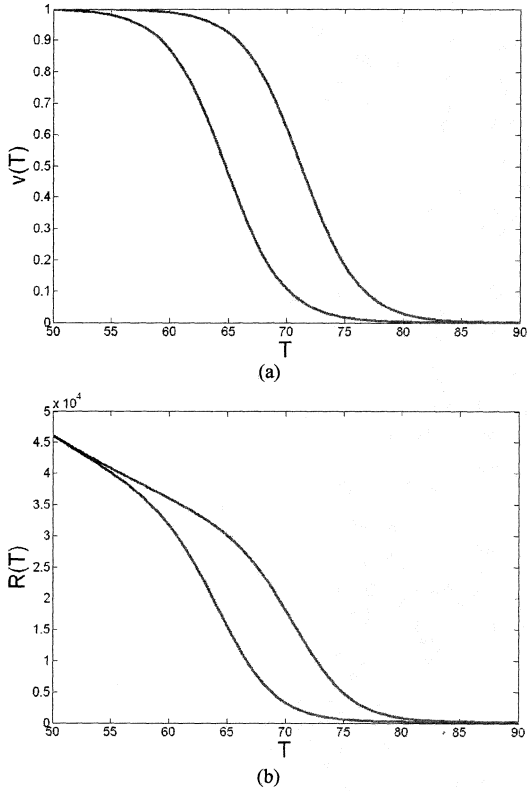

Fig. 1. (a) *υ(T)* and (b) *R(T)* major loop for Tc= 68 °C, w=6.5 °C

B. Incorporating minor loops

To incorporate minor loops, (6) can be modified with (2) to attain (7) where T_{pr} is the proximity temperature at reversal temperature point T_r. It should be noticed that for the case of major loop, $T_{pr} = w$ at any reversal point.

$$\gamma = \delta \frac{w}{2} + Tc - T + T_{pr}\ P(x) \quad (7)$$

$$x = \frac{T - T_r}{T_{pr}} \quad (8)$$

$$T_{pr} = \gamma_r - \frac{1}{\beta_g} \arctan(2\upsilon_r - 1) \quad (9)$$

$$P(x) = 0.5(1 - \sin \xi x)\left[1 + \tanh(\pi^2 - 2\pi x)\right] \quad (10)$$

Here, $\gamma_r = \gamma(T_r)$ and $\upsilon_r = \upsilon(T_r)$ as in (6) and (5) consecutively. T_{pr} and γ_r are changed only at the reversal point T_r and remain unchanged until the next reversal point. Is should be mentioned that for calculating υ_r at T_r, T_{pr} takes the value of T_{pr} ($T_r - \delta\ \Delta T$), which is basically the value of T_{pr} before the reversal point. Fig.2 (a-d) demonstrates the $\upsilon(T)$ and $R(T)$ loops where the T_{r1} =72 °C and T_{r2}=62 °C.

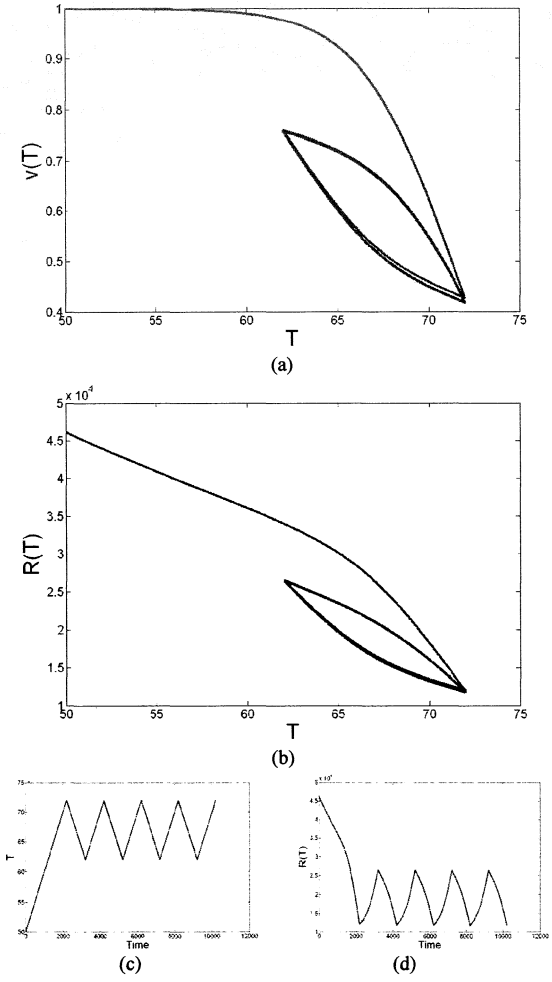

Fig. 2. (a) $\upsilon(T)$ and (b) *R(T) major and minor loops* for Tc= 68 °C, w=6.5 °C and T_{r1} =72 °C and T_{r2}=62 °C (c) shows the variation of T with time and the corresponding change of $R(T)$ is presented in (d).

For smaller change in temperature, T_{r1} =72 °C and T_{r2}=67 °C and the corresponding $\upsilon(T)$ and $R(T)$ loops are presented in Fig. 3(a-d)

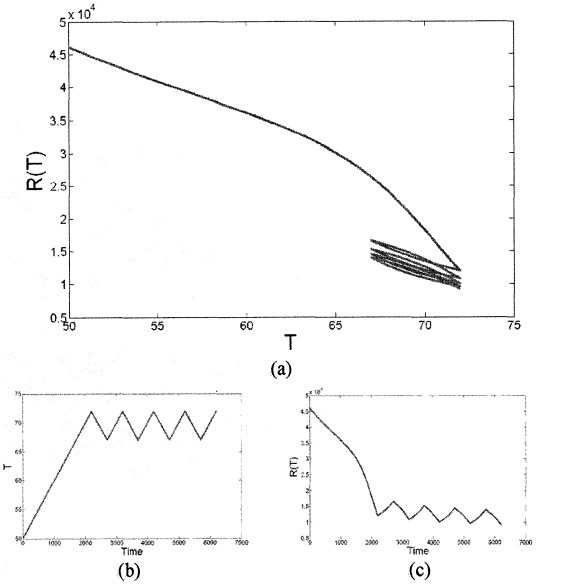

Fig. 3. (a) $\upsilon(T)$ and (b) *R(T) major and minor loops* for Tc= 68 °C, w=6.5 °C and T_{r1} =72 °C and T_{r2}=67 °C (c) shows the variation of T with time and the corresponding change of $R(T)$ is presented in (d).

It can be seen from Fig. 2 that the minor loops are stabilized readily for large minor loops while Fig. 3 shows that minor loops become stabilized after few cycles. The stabilization time is inversely proportional to the area of minor loops in R-T plane. Fig. 2 and Fig. 3 explain the loop accommodation process in VO_x.

C. *Nonsymmetrical hysteresis modeling*

In order to realize nonsymmetrical hysteresis behavior, the hysteresis width w can be modified to express the ascending loop as (13).

$$w_{-} = 0.5\, w_1 \left[1 - \tanh(\beta_{g-}(Tc - T))\right] + w_2 \quad (11)$$

Here $w_1$and w_2 depend on the limiting values of w_{-}. Fig. 4 shows the $\upsilon(T)$ and $R(T)$ major loops for nonsymmetrical case.

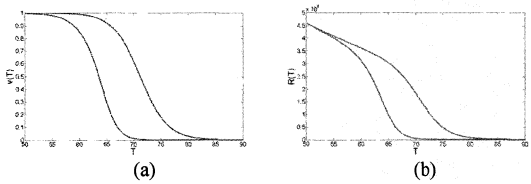

Fig. 4. (a) $\upsilon(T)$ and (b) $R(T)$ major loops for nonsymmetrical hysteresis case.

D. *Responsivity*

The voltage responsivity (R_v) is expressed in (12) where G_{th} is thermal conductance, V_B is bias voltage, η is absorbance and τ_{th} is thermal time constant. R_{dT} is expressed in (13). Fig. 5 shows that the responsivity is increased by a factor of 3 when the bolometer is operated in the hysteretic region.

$$R_v = \frac{\eta V_B R_{dt}}{G_{th}\sqrt{1+(2\pi f \tau_{th})^2}} \quad (12)$$

$$R_{dT} = R_{T+\Delta T} - R_T \quad (13)$$

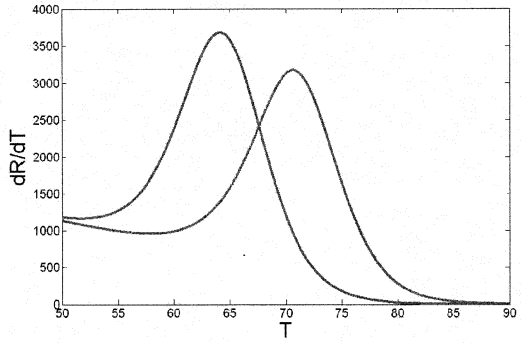

Fig. 5. R_{dT} for major ascending and descending loop; corresponds to normalized responsivity expressed in (12). For the descending loop, peak is observed at 70.66 °C.

V. Conclusion

VO_x materials are extremely promising for room temperature THz applications. Higher TCR can be achieved by high quality VO_x films, even with multilayer and doped films. The hysteresis width can also be minimized by fabrication process. NETD can be reduced by introducing on-chip readout circuit (ROIC). The main challenge is to operate the VO_x bolometer in the hysteretic region at suitable operating point to attain high TCR. Considering the thermal conductance (G_{th}) and thermal time constant (τ_{th}), Peltier elements can be used to cool down and heat up the bolometer to the optimum operating point.

References

[1] P. C. Shan, Z. Celik-Butler, D. P. Butler, A. Jahanzeb, C. M. Travers, W. Kula, and R. Sobolewski, "Investigation of semiconducting YBaCuO thin films: A new room temperature bolometer," *Journal of Applied Physics*, vol. 80, pp. 7118-23, 1996.

[2] M. E. MacDonald and E. N. Grossman, "Niobium microbolometers for far-infrared detection," *IEEE Transactions on Microwave Theory and Techniques*, vol. 43, pp. 893-6, 1995.

[3] V. K. Grunin, "Mathematical modeling of the temperature dependence of the parameters of uncooled metal bolometers," *Journal of Optical Technology*, vol. 68, pp. 952-5, 2001.

[4] N. Oda, Y. Tanaka, T. Sasaki, A. Ajisawa, A. Kawahara, and S. Kurashina, "Performance of 320 x 240 bolometer-type uncooled infrared detector," *NEC Research and Development*, vol. 44, pp. 170-174, 2003.

[5] C. Changhong, Y. Xinjian, Z. Xingrong, and X. Bifeng, "Preparation and properties of vanadium dioxide thin films for uncooled microbolometer," Beijing, China, 2000.

[6] V. Y. Zerov, Y. V. Kulikov, V. N. Leonov, V. G. Malyarov, I. A. Khrebtov, and I. I. Shaganov, "Features of the operation of a bolometer based on a vanadium dioxide film in a temperature interval that includes a phase transition," *Journal of Optical Technology*, vol. 66, pp. 387-90, 1999.

[7] H. Yong-Hee, C. In-Hoon, K. Ho-Kwan, P. Jong-Yeon, K. Kun-Tae, S. Hyun-Joon, and M. Sung, "Fabrication of vanadium oxide thin film with high-temperature coefficient of resistance using $V_2O_5/V/V_2O_5$ multi-layers for uncooled microbolometers," *Thin Solid Films*, vol. 425, pp. 260-4, 2003.

[8] J. T. W. I. William J. Parrish, Glenn T. Kincaid, Jeffery L. Heath, and Jeffery D. Frank "Low-cost 160 x 128 uncooled infrared sensor array," *Proceedings of SPIE, Infrared Readout Electronics IV*, vol. 3360, pp. 111-119, 1998.

[9] D. S. Tezcan, S. Eminoglu, O. S. Akar, and T. Akin, "A low cost uncooled infrared microbolometer focal plane array using the CMOS n-well layer," Interlaken, 2001.

[10] T. D. Manning, I. P. Parkin, M. E. Pemble, D. Sheel, and D. Vernardou, "Intelligent window coatings: atmospheric pressure chemical vapor deposition of tungsten-doped vanadium dioxide," *Chemistry of Materials*, vol. 16, pp. 744-9, 2004.

[11] A. Liebsch, H. Ishida, and G. Bihlmayer, "Coulomb correlations and orbital polarization in the metal-insulator transition of VO_2," *Physical Review B (Condensed Matter and Materials Physics)*, vol. 71, pp. 85109-1, 2005.

[12] R. M. Bowman and J. M. Gregg, "VO_2 thin films: growth and the effect of applied strain on their resistance," *Journal of Materials Science: Materials in Electronics*, vol. 9, pp. 187-91, 1998.

[13] J. Livage, G. Guzman, F. Beteille, and P. Davidson, "Optical properties of sol-gel derived vanadium oxide films," Faro, Portugal, 1997.

[14] M. Borek, F. Qian, V. Nagabushnam, and R. K. Singh, "Pulsed laser deposition of oriented VO_2 thin films on R-cut sapphire substrates," *Applied Physics Letters*, vol. 63, pp. 3288-90, 1993.

[15] P.-R. Zhu, S. Yamamoto, A. Miyashita, and H. Naramoto, "Pulsed laser deposition of VO_2 single crystal thin films on sapphire substrates," *Chinese Physics Letters*, vol. 15, pp. 904-6, 1998.

[16] H. Liu, O. Vasquez, V. R. Santiago, L. Diaz, A. J. Rua, and F. E. Fernandez, "Novel pulsed-laser-deposition - VO_2 thin films for ultrafast applications," Charlotte, NC, USA, 2005.

[17] D. Brassard, S. Fourmaux, M. Jean-Jacques, J. C. Kieffer, and M. A. El Khakani, "Grain size effect on the semiconductor-metal phase transition characteristics of magnetron-sputtered VO_2 thin films," *Applied Physics Letters*, vol. 87, pp. 51910-1, 2005.

[18] X. Shiqing, M. Hongping, D. Shixun, and J. Zhonghong, "Study on optical and electrical switching properties and phase transition mechanism of Mo^{6+}-doped vanadium dioxide thin films," *Journal of Materials Science*, vol. 39, pp. 489-93, 2004.

[19] M. A. Abdullaev, I. K. Kamilov, and E. I. Terukov, "Preparation and properties of stoichiometric vanadium oxides," *Inorganic Materials*, vol. 37, pp. 271-3, 2001.

[20] G. Obermeier, D. Ciesla, S. Klimm, and S. Horn, "Pressure dependence of phase transitions in the quasi-one-dimensional metal-insulator transition system β-$Na_{1/3}V_2O_5$," *Physical Review B (Condensed Matter and Materials Physics)*, vol. 66, pp. 85117-1, 2002.

[21] F. Beteille and J. Livage, "Optical switching in VO_2 thin films," Sheffield, UK, 1998.

[22] D. H. Kim and H. S. Kwoka, "Pulsed laser deposition of VO_2 thin films," *Applied Physics Letters*, vol. 65, pp. 3188-90, 1994.

[23] F. Guinneton, L. Sauques, J. C. Valmalette, F. Cros, and J. R. Gavarri, "Comparative study between nanocrystalline powder and thin film of vanadium dioxide VO_2: electrical and infrared properties," *Journal of the Physics and Chemistry of Solids*, vol. 62, pp. 1229-38, 2001.

[24] C. D. Reintsema, E. N. Grossman, and J. A. Koch, "Improved VO_2 microbolometers for infrared imaging: operation on the semiconducting-metallic phase transition with negative electrothermal feedback," Orlando, FL, USA, 1999.

[25] L. A. L. de Almeida, G. S. Deep, A. M. N. Lima, and H. Neff, "Limiting loop proximity hysteresis model," *IEEE Transactions on Magnetics*, vol. 39, pp. 523-8, 2003.